High Pressure Synthesis of $NdCuO_{3-\delta}$ Perovskites ($0 \leq \delta \leq 0.5$)

Bai-Hao Chen* and Dave Walker

Lamont-Doherty Earth Observatory of Columbia University, Palisades, New York 10964

Emmanuelle Suard and Bruce A. Scott

IBM Thomas J. Watson Research Center, Yorktown Heights, New York 10598

Bernard Mercey, Maryvonne Hervieu, and Bernard Raveau

CRISMAT, University of Caen, Caen, France

Received September 16, 1994[⊗]

Oxygen-deficient perovskites $NdCuO_{3-\delta}$ ($0 \leq \delta \leq 0.5$) were prepared for the first time at high pressures in a multianvil apparatus and characterized by X-ray and electron diffraction and by electron microprobe. Several new oxygen vacancy-order phases could be stabilized depending upon δ and synthetic conditions. The crystal structures of $NdCuO_{3-\delta}$ are related to those previously observed in the $LaCuO_{3-\delta}$ system, but are more highly distorted due to the smaller Nd cation size, leading to different symmetries, A-site coordination numbers and unit cell dimensions. Electron diffraction shows that $NdCuO_{2.5}$ crystallizes in an orthorhombic $\sqrt{2}a_p \times 2\sqrt{2}a_p \times a_p$ subcell with a $6\sqrt{2}a_p \times 4\sqrt{2}a_p \times 2a_p$ supercell, where a_p is the simple cubic perovskite lattice parameter. $NdCuO_{2.6}$ crystallizes in a monoclinic $\sqrt{5}a_p \times \sqrt{5}a_p \times 2a_p$ cell. In addition, two other phases with $\sqrt{10}a_p \times \sqrt{10}a_p \times 2a_p$ and $\sqrt{5}a_p \times 2\sqrt{5}a_p \times 2a_p$ have been observed for $\delta = 0.3-0.4$, each exhibiting superstructures related to $NdCuO_{2.6}$. Oxygen vacancy ordering models are proposed to interpret these results. An orthorhombic $GdFeO_3$-type phase with $\delta = 0-0.07$, the first example of this structure-type in the rare earth cuprates, was found at the highest oxygen pressures investigated. The major structure-types, corresponding to $\delta = 0.07$, 0.4, and 0.5, were refined by the Rietveld method. It was not possible to synthesize other $LnCuO_{3-\delta}$ phases for rare earths smaller than Nd at pressures up to 150 kbar. Superconductivity was not observed in any of the new perovskites down to 4.2 K.

Introduction

High pressures are required to synthesize perovskite rare earth cuprates. Oxygen-deficient perovskites $LaCuO_{3-\delta}$ have been prepared at oxygen pressures from 0.2 to 1 kbar using coprecipitated La and Cu hydroxide precursors.[1-4] Three types of oxygen-deficient structures were found in this system. Orthorhombic $LaCuO_{2.5}$ (225-type, $0.43 \leq \delta \leq 0.5$) exhibits the orthorhombic $CaMnO_{2.5}$ structure-type,[5,6] with $a \approx \sqrt{2}a_p$, $b \approx 2\sqrt{2}a_p$, and $c \approx a_p$, where a_p is the simple perovskite subcell parameter. Monoclinic $LaCuO_{2.6}$ (5-5-13) exhibits a structure similar to tetragonal $La_4BaCu_5O_{13}$[7] and $(La,Sr)_5Cu_5O_{13}$,[8] with $a \approx \sqrt{5}a_p$, $b \approx \sqrt{5}a_p$, $c \approx a_p$, and $\gamma \approx 90°$. In both 225 and 5-5-13, oxygen-vacancy ordering leads to an array of parallel pseudohexagonal tunnels. In addition, the Cu(II) and Cu(III) cations reside in distorted corner-sharing square pyramidal and octahedral sites, respectively. A third structure-type, $LaCuO_{3-\delta}$ (113 phase, $0 \leq \delta \leq 0.2$) is observed at pressures of 1 kbar and higher.[1,9] It is tetragonal with $a \approx a_p$ and $c \approx a_p$, but transforms slowly to a rhombohedral perovskite of the $LaNiO_3$-type above 60 kbar.[9-11] A Rietveld refinement of neutron diffraction data suggests that the rhombohedral phase can exist with oxygen contents as low as $LaCuO_{2.88}$.[12] Rhombohedral $LaCuO_3$ has been reported to transform to yet another tetragonal structure with $a \approx \sqrt{2}a_p$ and $c \approx 2a_p$ on heating to 408 °C.[11] Attempted preparation of the other $LnCuO_3$ (Ln = rare earth metal) at 900 °C and 65 kbar was unsuccessful.[10] The $LaCuO_{3-\delta}$ phases are metallic over the composition range $0 \leq \delta \leq 0.4$, but superconductivity was not observed in this system down to 4.2 K, most likely because the oxygen vacancy ordering is not two-dimensional.[2] Other rare earth metal cuprates of 225 composition are known for Ln = Y, Tb−Lu, but they do not exhibit structures related to perovskite.[13-15] This

[⊗] Abstract published in *Advance ACS Abstracts,* March 15, 1995.

(1) Bringley, J. F.; Scott, B. A.; La Placa, S. J.; Boehme, R. F.; Shaw, T. M.; McElfresh, M. W.; Trail, S. S.; Cox, D. E. *Nature* **1990**, *347*, 263.
(2) Bringley, J. F.; Scott, B. A.; La Placa, S. J.; McGuire, T. R.; Mehran, F.; McElfresh, M. W.; Cox, D. E. *Phys. Rev. B* **1993**, *47*, 15269.
(3) La Placa, S. J.; Bringley, J. F.; Scott, B. A.; Cox, D. E. *Acta Crystallogr., Sect. C* **1993**, *49*, 1415.
(4) La Placa, S. J.; Bringley, J. F.; Scott, B. A.; Cox, D. E. *Acta Crystallogr., Sect. C*, in press.
(5) Poeppelmeier, K. R.; Lenowicz, J. E.; Longo, J. M. *J. Solid State Chem.* **1982**, *44*, 89.
(6) Poeppelmeier, K. R.; Lenowicz, M. E.; Scanlon, J. C.; Longo, J. M.; Yelon, W. B. *J. Solid State Chem.* **1982**, *45*, 71.
(7) Michel, C.; Er-Rakho, L.; Hervieu, M.; Pannetier, J.; Raveau, B. *J. Solid State Chem.* **1987**, *68*, 143.
(8) Otzschi, K.; Hayashi, A.; Fujiwara, Y.; Ueda, Y. *J. Solid State Chem.* **1993**, *105*, 573.
(9) Darracq, S.; Largeteau, A.; Demazeau, G.; Scott, B. A.; Bringley, J. F. *Eur. J. Solid State Inorg. Chem.* **1992**, *29*, 585.
(10) Demazeau, G.; Parent, C.; Pouchard, M.; Hagenmuller, P. *Mater. Res. Bull.* **1972**, *7*, 913.
(11) Webb, A. W.; Skelton, E. F.; Qadri, S. B.; Carpenter, E. R.; Osofsky, Jr. M. S.; Soulen, R. J.; Letourneau, V. *Phys. C* **1989**, *162*, 899.
(12) Currie, D. B.; Weller, M. T. *Acta Crystallogr., Sect. C* **1991**, *47*, 696.

0020-1669/95/1334-2077$09.00/0

is also true for monoclinic $LaCuO_{2.5}$,[16] and hexagonal $YCuO_{2.5+x}$ and $LaCuO_{2.5+x}$.[17]

The key feature of the cuprate superconductors is the ordering of oxygen vacancies into two-dimensional sheets within the perovskite framework, and rare earth metal cation ordering plays a major role in stabilizing such structures.[18,19] For this reason, an understanding of the structure-stability relationships in the $LnCuO_{3-\delta}$ systems is important in defining synthetic strategies for creating new vacancy-ordered cuprates at high pressures.[20] In this paper, we report an investigation of possible perovskite fields in $LnCuO_{3-\delta}$ systems for Ln = Y, Nd, Sm, and Gd to pressures of 150 kbar. Five new perovskite-type phases were observed in the $NdCuO_{3-\delta}$ system and their compositions and crystal structures were determined by electron microprobe, electron and X-ray powder diffraction, and refined by Rietveld profile analysis.[21]

Experimental Section

A coprecipitation technique similar to that used for the synthesis of the perovskite series $LaCuO_{3-\delta}$[22] was applied to prepare the precursors for high pressure synthesis of the $LnCuO_{3-\delta}$ phases (Ln = Y, Nd, Sm and Gd; $0 \leq \delta \leq 0.5$). Ln_2O_3 (0.001 mol) and CuO (0.002 mol) powders (Alfa) were dissolved in 1 M HNO_3 (40 mL) by gentle heating and stirring. The solution was diluted to 100 mL with H_2O and cooled by stirring in an ice bath to 5 °C. Aqueous NaOH (3 M) was then added with stirring until a blue precipitate appeared (pH ~9). It was filtered and thoroughly washed with H_2O to remove sodium, placed in a platinum crucible and heated in air at 700−850 °C for 20 h.

The resulting precursor had an overall 225 stoichiometry, but was single phase only for $Y_2Cu_2O_5$. The larger rare earths gave precursors which were mixtures of CuO and the 214 phase, i.e., CuO + Ln_2CuO_4. Firing the mixtures at temperatures below 800 °C yielded fine-grained precursors, which was important to achieving equilibrium phase assemblages in single high pressure synthesis experiments. For experiments at 100 kbar, the precursors were mixed and ground with the desired amount of $KClO_3$ to fix the oxygen content, packed into 2.5 mm i.d. × 6 mm long Al_2O_3 crucibles, and loaded into a ceramic octahedron with a truncated edge length (TEL) of 8 mm. For experiments above 100 kbar, 2.5 mm i.d. × 4 mm long crucibles were employed with 6 mm TEL octahedra serving as the pressure media. The assemblies were also fitted with $LaCrO_3$ sleeves, which functioned as heaters, and W 3% Re/W 25% Re thermocouples. A full description of the multianvil apparatus and the high pressure experimental procedures has been published previously.[23]

Samples were characterized with a Siemens D500 X-ray powder diffractometer with monochromator using Cu Kα radiation. The X-ray powder data were obtained in the range $4° < 2\theta < 70°$ using a step width of 0.02° and a counting time of 20 s. All structural parameters for the new phases were refined by the Fullprof Rietveld program[24] using a pseudo-Voigt peak-shape function. The refined parameters include atom positions, lattice parameters, a zero point error, isotropic parameters, overall scale factor, peak-shape parameter, full-width parameters, and background parameters. Electron diffraction (ED) studies were carried out with a Philips EM-420 electron microscope operating at 120 kV.

Table 1. Summary of Relationship between the Lattice Parameters for $LnCuO_{3-\delta}$ (Ln = La,[1] Nd) and a Lattice Parameter a_p for Simple Cubic Perovskite

composition	sample no.	$a(a_p)$	$b(a_p)$	$c(a_p)$	γ (deg)
$LaCuO_{2.5}$		$\sqrt{2}$	$2\sqrt{2}$	1	90.0
$NdCuO_{2.5}$	I	$6\sqrt{2}$	$4\sqrt{2}$	2	90.0
$LaCuO_{2.6}$		$\sqrt{5}$	$\sqrt{5}$	1	90.2
$NdCuO_{2.6}$	II, III	$\sqrt{5}$	$\sqrt{5}$	2	90.5
$NdCuO_{3-\delta}$ ($\delta = 0.3-0.4, \alpha$)	II, III	$\sqrt{10}$	$\sqrt{10}$	2	90.5
$NdCuO_{3-\delta}$ ($\delta = 0.3-0.4, \beta$)	II	$\sqrt{5}$	$2\sqrt{5}$	2	90.5
$LaCuO_{2.95}$		1	1	1	90.0
$NdCuO_{2.93}$	III, IV	$\sqrt{2}$	$\sqrt{2}$	2	90.0

A CAMEBAX electron microprobe was used to measure sample compositions. Operating conditions for 1−2 μm focused beams typically were 15 kV accelerating voltage and 50 nA beam current. Wavelength-dispersive analysis of the Kα lines of Cu and O and the Lα line of Nd were undertaken with LiF, lead stearate, and PET crystals. Backgrounds were collected at wavelengths both above and below all peaks. Peak and background counting times were chosen to give 0.5% reproducibility in the counting statistics. This expected precision was confirmed by replicate analysis of the standard. Very clean, single-phase $Nd_2Cu_2O_5$, a product of one of our experiments, was used as the standard for all three elements. This material was chosen as the standard to be very close in composition to the unknown—the only chemical difference between the standard and some of the samples being the oxygen content. The oxygen content of the $Nd_2Cu_2O_5$ standard is accurately known as it was prepared as a single phase at that composition from known precursors and checked by reduction in a TGA apparatus. Further, confirmation of the oxygen stoichiometry in our $Nd_2Cu_2O_5$ standard and the adequacy of the Cameca PAP correction procedures used to reduce the data were obtained by recovering within analytical precision the correct stoichiometry in analysis of CuO, Nd_2O_3, and $NdCu_2O_4$. Oxygen occurs in a range of coordinations in these compounds. Evidently, the broadness of the peak on the lead stearate analyzing crystal makes potential oxygen peak shifts unimportant.

Results and Discussion

Synthesis of $LnCuO_{3-\delta}$ phases were attempted for $\delta = 0$ and 0.5 with Ln = Y, Gd, Sm and Nd, but only the latter yielded materials with perovskite-related structures. For the others, X-ray powder data show that the final products of synthesis were CuO and T′-type Ln_2CuO_4,[25,26] or more complex unknown phases whose compositions depend on oxygen content.[27]

On the basis of these results, work centered on the $NdCuO_{3-\delta}$ system. A series of 100 kbar/1000 °C synthesis runs was carried out by systematically varying the oxygen content from $\delta = 0$ to 0.5. Three new phases were identified by X-ray diffraction; however, closer inspection of the assemblages by ED and EM showed that four different compositions actually occur in five different oxygen vacancy-ordered structures over this composition range. These are shown in Table 1. The results obtained from the tabulated samples are typical of that found in over twenty separate runs in the series. Sample I ($NdCuO_{2.5}$) was

(13) Freund, H.-R.; Müller-Buschbaum, Hk. *Z. Naturforsch.* **1977**, *32B*, 609.
(14) Freund, H.-R.; Müller-Buschbaum, Hk. *Z. Naturforsch.* **1977**, *32B*, 1123.
(15) Okada, H.; Takano, M.; Takeda, Y. *Phys. C* **1990**, *166*, 111.
(16) Cava, R. J.; Siegrist, T.; Hessen, B.; Krajewski, J. J.; Peck, W. F., Jr.; Batlogg, B.; Takagi, H.; Waszczak, J. V.; Schneemeyer, L. F.; Zandbergen, H. W. *J. Solid State Chem.* **1991**, *94*, 170.
(17) Cava, R. J.; Zandbergen, H. W.; Ramirez, A. P.; Takagi, H.; Chen, C. T.; Krajewski, J. J.; Peck, Jr., W. F.; Waszczak, V.; Meigs, G.; Roth, R. S.; Schneemeyer, L. F. *J. Solid State Chem.* **1993**, *104*, 437.
(18) Raveau, B.; Michel, C.; Hervieu, M.; Groult, D. *Crystal Chemistry of High-T_c Superconducting Oxides*; Springer Series in Materials Science 15; Springer-Verlag: New York, **1991**.
(19) Anderson, M. T.; Vaughey, J. T.; Poeppelmeier, K. R. *Chem. Mater.* **1993**, *5*, 151.
(20) Guloy, A. M.; Scott, B. A.; Figat, R. A. *J. Solid State Chem.* **1994**, *113*, 54.
(21) Rietveld, H. M. *J. Appl. Cryst.* **1969**, *2*, 65.
(22) Bringley, J. R.; Scott, B. A. *Inorg. Synth.* **1993**, *73*, 246.
(23) Walker, D. *Am. Mineral.* **1991**, *76*, 1092.
(24) Rodriguez-Carvajal, J.; Fullprof: A Program for Rietveld refinement and profile matching analysis of complex powder diffraction patterns (ILL, unpublished).
(25) Müller-Buschbaum, H. K.; Wollschlager, W. *Z. Anorg. Allg. Chem.* **1975**, *414*, 76.
(26) Grand, B.; H. K.; Wollschlager, W.; Schweizer, M. *Z. Anorg. Allg. Chem.* **1977**, *428*, 120.
(27) Reller, A.; Jefferson, D. A.; Thomas, J. M.; Uppal, M. K. *J. Phys. Chem.* **1983**, *87*, 913.

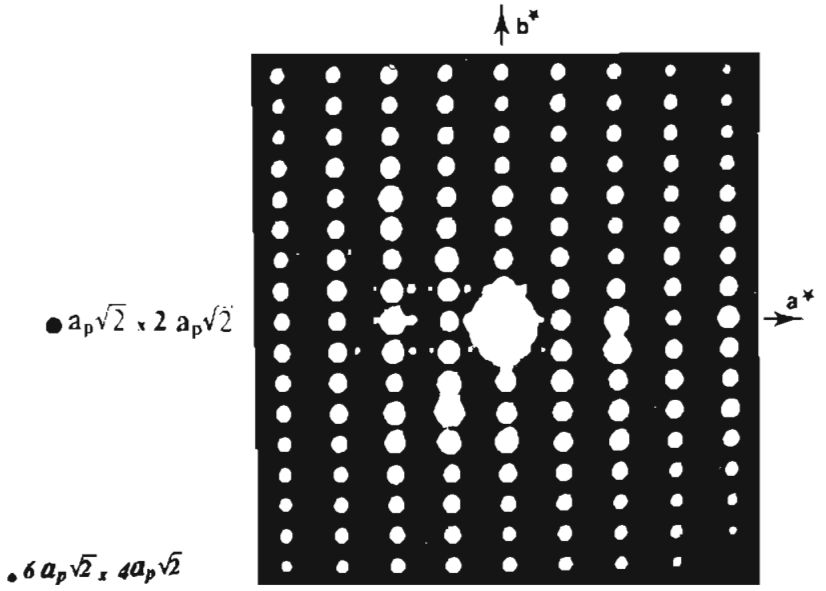

Figure 1. Electron diffraction pattern along [001] for $NdCuO_{2.5}$.

obtained from the 225 precursor after 30 h at 100 kbar and 1000 °C in the absence of $KClO_3$. Sample II was synthesized at the nominal composition $\delta = 0.375$ and was found to be $NdCuO_{2.63(3)}$ by electron microprobe using $NdCuO_{2.5}$ as a standard. Sample III was obtained from a nominally $\delta = 0.25$ composition in a 30 h run, at 100 kbar and 1000 °C, and also in a 5 day run at 100 kbar and 600 °C, and was comprised mostly of $NdCuO_{2.70(3)}$. Another new phase, $NdCuO_{2.93}$, was also present in sample III; however, it was best prepared by reacting the 225 precursor with excess $KClO_3$ ($\delta = -0.25$) at 1000 °C and 100/150 kbar. The results below were obtained on a sample synthesized at 150 kbar (sample IV). As suggested by Table 1, $NdCuO_{2.63(3)}$ and the two forms of $NdCuO_{3-\delta}$ ($0.3 \leq \delta \leq 0.4$) were very difficult to synthesize as pure phases; furthermore, they could not be easily distinguished by X-ray diffraction because of their structural similarities.

Electron Diffraction Study. Electron diffraction patterns along [001], which revealed the different superstructures of simple cubic perovskite for the $NdCuO_{3-\delta}$ samples described above, are shown in Figures 1 and 2. A summary of the relationship between the crystallographic cells of $LnCuO_{3-\delta}$ (Ln = La and Nd) and that of simple cubic perovskite based on the ED patterns and the results of previous work[1] is given in Table 1.

Figure 1 shows an ED pattern observed in I ($NdCuO_{2.5}$). The weak spots in the pattern exhibit a supercell $6\sqrt{2}a_p \times 4\sqrt{2}a_p$, while the strong spots correspond to $\sqrt{2}a_p \times 2\sqrt{2}a_p$. The unit cell dimensions of the latter are similar to those observed in the orthorhombic $LaCuO_{2.5}$, but the $NdCuO_{2.5}$ reflections have violations of the $LaCuO_{2.5}$ space group *Pbam*.[1,3] However, the larger supercell reflections for $NdCuO_{2.5}$ were not observed by X-ray diffraction. These reflections are probably too weak, or possibly due to a slightly different oxygen content. For these reasons, the X-ray diffraction data for $Nd_2Cu_2O_5$ were refined on the basis of the $La_2Cu_2O_5$ model.

Samples II and III exhibit ED patterns due to two different unit cells, as shown in Figure 2a,b. The first corresponds to $\sqrt{5}a_p \times \sqrt{5}a_p$, while the second is twice as large, $\sqrt{10}a_p \times \sqrt{10}a_p$ (α-type). Another cell of dimension $\sqrt{5}a_p \times 2\sqrt{5}a_p$ (β-type) was only observed in sample II (see Figure 2c). These cells are connected to monoclinic $NdCuO_{2.6}$ through the relationships $a_m \times b_m$, $\sqrt{2}a_m \times \sqrt{2}b_m$ and $a_m \times 2b_m$ of monoclinic $LaCuO_{2.6}$, where a_m and b_m are the lattice parameters of $LaCuO_{2.6}$. The γ angle is very close to 90° in these phases and could not be measured by electron diffraction. Their monoclinic symmetries were confirmed by X-ray diffraction.

Several structural models, represented schematically in Figure 3, are presented to interpret the results. The model for $NdCuO_{2.6}$ is depicted in Figure 3a and is equivalent to the 5-5-13 structure of monoclinic $LaCuO_{2.6}$. The three models proposed for the α- and β-type supercells are shown in Figure 3b–d. These are based on alternate intergrowths of $NdCuO_{2.6}$- (5-5-13) and $NdCuO_{2.8}$-type (5-5-14) slabs along [100]. Although a phase of composition $NdCuO_{2.8}$ was not observed in this work, a possible $CaMnO_{2.8}$-type (5-5-14) ordering scheme[27] for it is depicted in Figure 3e. In this arrangement, each $Cu^{III}O_6$ octahedron is linked by corner-sharing with two $Cu^{II}O_5$ square pyramids and four $Cu^{III}O_6$ octahedra. The first 10-10-27 model (α-type) for $NdCuO_{2.7}$ corresponds to the $\sqrt{10}a_p \times \sqrt{10}a_p$ cell of Figure 3b. The structure is similar to that of $La_4BaCu_5O_{13+x}$.[7] Parts c and d of Figure 3 illustrate 10-10-27 structure types denoted $\beta(a)$ and $\beta(b)$, respectively. They are both related to a $\sqrt{5}a_p \times 2\sqrt{5}a_p$ cell with different stacking sequences, observed for the first time in perovskites. The $\sqrt{5}a_p \times 2\sqrt{5}a_p$ cell (β-type), was found only in samples prepared and quenched from 100 kbar and 1000 °C (sample II). This suggests that α and β could be low and high temperature forms of $NdCuO_{2.7}$ respectively.

In contrast to the $LaCuO_{3-\delta}$ series, a doubled lattice parameter in the c-axis, normal to the oxygen-vacancy ordered planes was observed in all $NdCuO_{3-\delta}$ phases. This effect could be caused by a slight distortion of either the CuO_2 or NdO layers, causing the cations and oxygens to be noncoplanar.

X-ray Powder Diffraction Study. As previously discussed, supercells related to the structures of $LaCuO_{2.5}$ and $LaCuO_{2.6}$ were observed by electron diffraction of the Nd-cuprate phases. However, no extra reflections corresponding to these supercells were observed in their X-ray diffraction patterns. In order to limit the number of refinement parameters, the smallest subcells which produced the strongest ED reflections were chosen for Rietveld refinement. Therefore, the structures of $NdCuO_{2.5}$ (sample I) and $NdCuO_{2.6}$ (sample II) were refined in the space groups of their lanthanum analogs.[3,4] The X-ray data in impurity regions were excluded from the refinement. The $NdCuO_{2.93}$

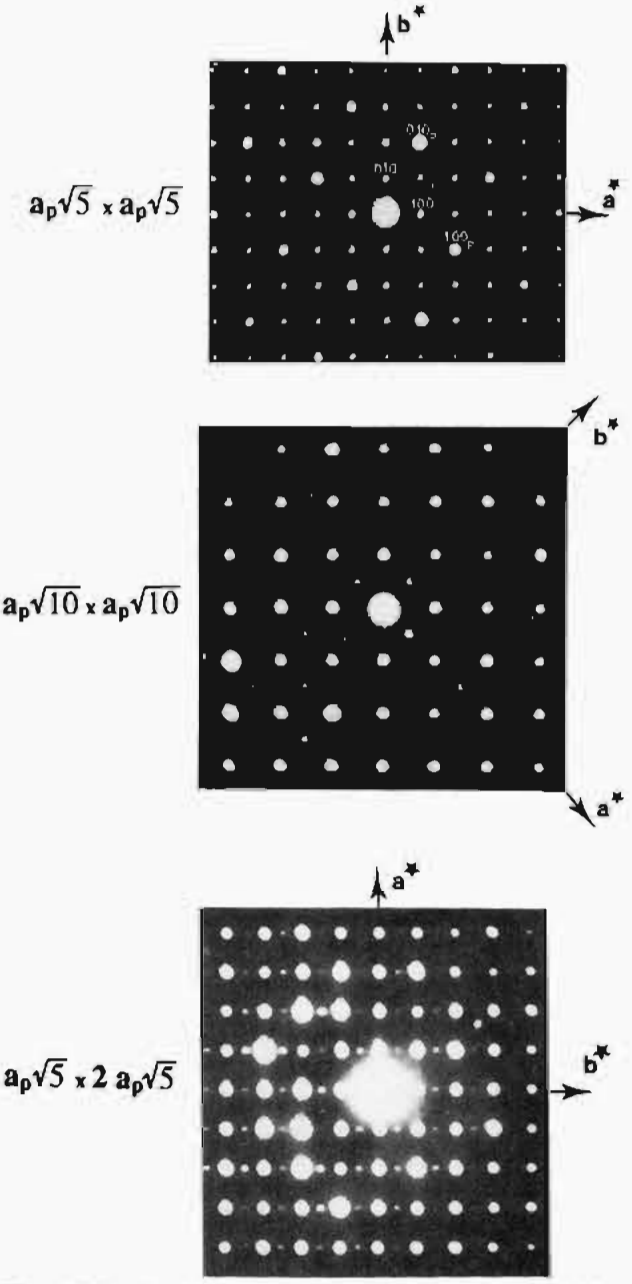

Figure 2. Electron diffraction patterns along [001] for (a) $NdCuO_{2.6}$, (b) α-type (strong spots: $\sqrt{5}a_p \times \sqrt{5}a_p$), and (c) β-type (strong spots: $\sqrt{5}a_p \times \sqrt{5}a_p$).

(sample IV) phase, on the other hand, has no direct La analog. Because of the similarity of its X-ray pattern to $NdTiO_3$,[28] this structure was used as the initial model for refinement. The KCl second phase in the $NdCuO_{2.93}$ sample was also included in the Rietveld refinement. The calculated and observed X-ray patterns are depicted in Figure 4, and a summary of crystallographic data from the Rietveld refinements are given in Table 2.

Structure of $NdCuO_{2.5}$. Orthorhombic $NdCuO_{2.5}$ is isostructural to $LaCuO_{2.5}$ and $CaMnO_{2.5}$ with Pbam symmetry[5,6] and the strongest ED reflections are produced by the $\sqrt{2}a_p \times 2\sqrt{2}a_p \times a_p$ unit cell. The Rietveld refinement was therefore performed in this space group and the results are given in Table 2. The relatively high R_{wp} in the refinement could be due to the very small sample available for measurement and the presence of superstructure. Small amounts of impurity phases present in the pattern (Figure 4) may also contribute. However, the S_{wp} value is acceptable. Note that the a parameter of $NdCuO_{2.5}$ is greater than that of $LaCuO_{2.5}$, while both b and c are smaller (Table 2). The structure of $NdCuO_{2.5}$ is presented in Figure 5a, and the refined positional parameters and selected bond distances and angles are found in Table 3.

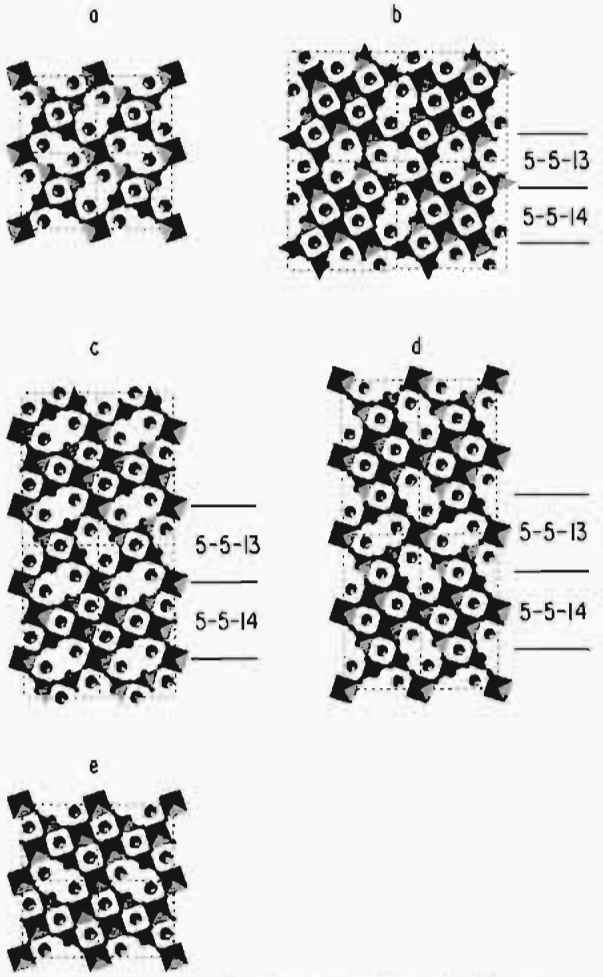

Figure 3. Structural models for (a) $NdCuO_{2.6}$ (5-5-13), (b) α-type $NdCuO_{2.7}$, (c and d) β-types $NdCuO_{2.7}$, and (e) "$NdCuO_{2.8}$" (5-5-14). Large, medium, and small balls represent Nd, Cu, and O atoms, respectively.

Table 2. Crystallographic Data for $NdCuO_{3-\delta}$[a]

formula cryst syst space group	$NdCuO_{2.5}$[a] orthorhombic *Pbam* (No. 55)	$NdCuO_{2.6}$[b] monoclinic *P2/m* (No. 10)	$NdCuO_{2.93}$ orthorhombic *Pbnm* (No. 62)
a (Å)	5.596(1)	8.560(2)	5.334(1)
b (Å)	10.29(2)	8.534(2)	6.308(1)
c (Å)	3.806(1)	3.777(1)	7.196(2)
γ deg	90.0	90.45(5)	90.0
V (Å^3)	219.1(1)	275.9(1)	242.2(1)
Z	4	5	4
D_{calc} (g/cm^3)	7.511	7.505	7.016
R_{wp} (%)	20.6	13.3	16.9
R_I (%)	9.34	5.36	7.96
R_e (%)	13.8	10.8	11.6
S_{wp}	1.49	1.23	1.46

[a] For comparison, $LaCuO_{2.5}$: a = 5.5490(1) Å, b = 10.4774(2) Å, c = 3.8796(1) Å. [b] For comparison, $LaCuO_{2.6}$: a = 8.62884(5) Å, b = 8.65148(5) Å, c = 3.83076(2) Å, γ = 90.2166(4)°. [c] $R_{wp} = \{\sum_n(Y_{obs} - Y_{cal})^2/[\sum_n(Y_{obs} - Y_{cal})^2/\sum(Y_{obs})^2]\}^{1/2}$. $R_I = \sum|I_{obs} - I_{cal}|/\sum I_{obs}$. $R_e = [(N - P)/\sum_n(Y_{obs})^2]^{1/2}$. $S_{wp} = R_{wp}/R_e$.

$NdCuO_{2.5}$ consists entirely of corner-sharing Cu(II)O_5 square pyramids. The ordered oxygen-vacancies create parallel tunnels where the Nd atoms reside. Nine oxygens surround each Nd atom, forming a distorted tricapped-trigonal prism with almost

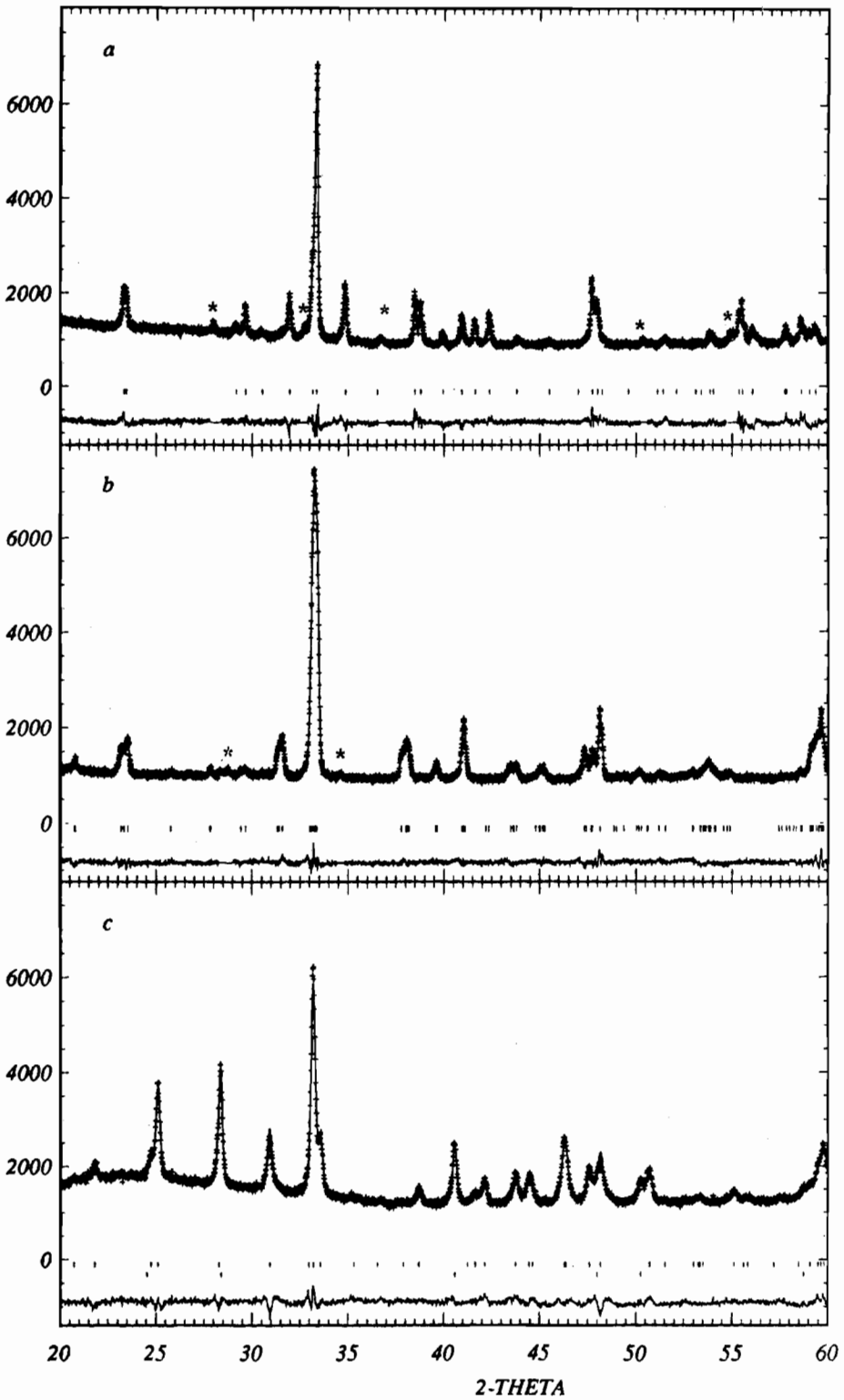

Figure 4. Rietveld refinement of powder X-ray diffraction data for (a) $NdCuO_{2.5}$, (b) $NdCuO_{2.6}$, and (c) $NdCuO_{2.93}$. Impurity peaks are marked with asterisks.

equal Nd−O distances ranging from 2.552 to 2.664 Å (see Figure 5b). This can also be visualized as an Nd atom occupying a triangular face shared by two distorted octahedra, with three oxygens above, three below, and three in the Nd plane. O(1) is too far away from Nd (3.037 Å) to coordinate to it. The average Nd−O distance of 2.615 Å is slightly shorter than the La−O distance of 2.691 Å in $LaCuO_{2.5}$, where each La atom is coordinated by 10 oxygens.[3] The CuO_5 square pyramid, like that found in $LaCuO_{2.5}$, contains four short Cu−O distances and one long Cu−O distance that is *trans* to the oxygen vacancy. However, the distortion of the pyramid in the former is greater than observed in $LaCuO_{2.5}$. The ratio of the long Cu−O distance and the average *short* Cu−O distance in $NdCuO_{2.5}$ is 1.22, compared to 1.16 for $LaCuO_{2.5}$. It would appear that the Cu atoms are tending toward CuO_4 square planar geometry. The O−Cu−O bond angles, which are 90° for the ideal cubic perovskite, range from 83.3 to 92.1° in $NdCuO_{2.5}$ compared to 87.2−92.5° for $LaCuO_{2.5}$.

Structure of $NdCuO_{2.6}$. Monoclinic $NdCuO_{2.6}$ (5-5-13 phase) is isostructural to $LaCuO_{2.6}$ with $P2/m$ symmetry, and

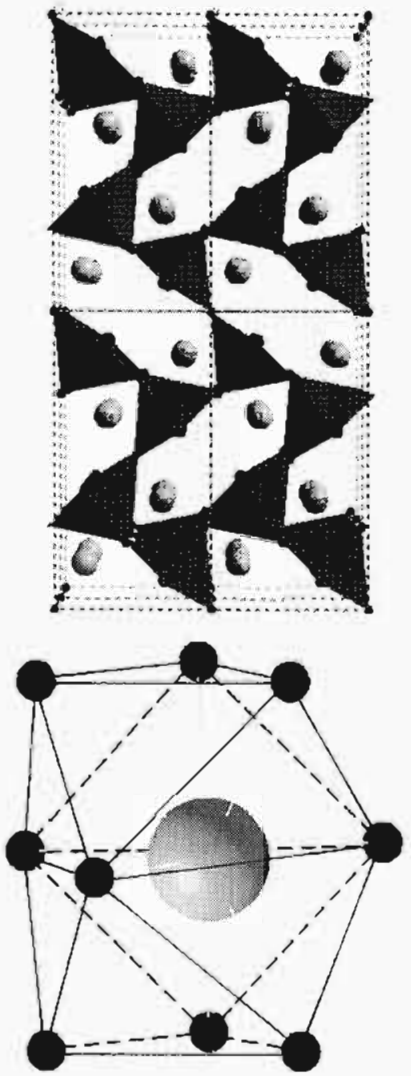

Figure 5. (a) Structure of $NdCuO_{2.5}$ projected on [001]. (b) NdO_9 coordination polyhedron in $NdCuO_{2.5}$. Large, medium, and small balls represent Nd, Cu, and O atoms, respectively.

Table 3. Positional Parameters and Selected Bond Distances (Å) and Angles (deg) for $NdCuO_{2.5}$

atom	site	x	y	z
Nd	4h	0.3224(4)	0.3564(3)	0.5
Cu	4g	0.2985(9)	0.0981(5)	0.0
O(1)	4b	0.281(3)	0.098(2)	0.5
O(2)	4g	0.543(3)	0.223(2)	0.0
O(3)	2a	0.0	0.0	0.0

Nd−O(1)	3.037(4) [1×]	O(1)−Cu−O(1)	174.0(2)
Nd−O(1)	2.664(4) [1×]	O(1)−Cu−O(2)	92.1(1)
Nd−O(1)	2.556(4) [1×]	O(1)−Cu−O(2)	88.1(1)
Nd−O(1)	2.607(4) [1×]	O(1)−Cu−O(3)	87.5(1)
Nd−O(2)	2.652(2) [2×]	O(2)−Cu−O(2)	84.7(1)
Nd−O(2)	2.594(2) [2×]	O(2)−Cu−O(3)	168.0(1)
Nd−O(3)	2.606(1) [2×]	O(2)−Cu−O(3)	83.31(9)
Cu−O(1)	1.906(1) [2×]		
Cu−O(2)	1.876(4) [1×]		
Cu−O(2)	2.331(4) [1×]		
Cu−O(3)	1.952(1) [1×]		

its $\sqrt{5}a_p \times \sqrt{5}a_p \times a_p$ unit cell is smaller than that of $LaCuO_{2.6}$ (Table 2). The slightly larger monoclinic angle in $NdCuO_{2.6}$ ($\gamma = 90.45°$) compared to $LaCuO_{2.6}$ ($\gamma = 90.22$) indicates that the former is somewhat more distorted.

The structure of $NdCuO_{2.6}$ is presented in Figure 6, while refined positional parameters and selected bond distances are

Figure 6. Structure of $NdCuO_{2.6}$ projected on [001]. Large, medium, and small balls represent Nd, Cu, and O atoms, respectively.

Table 4. Structural Parameters for $NdCuO_{2.6}$

(a) Positional Parameters

atom	site	x	y	z
Nd(1)	1h	0.5	0.5	0.5
Nd(2)	2n	0.1369(7)	0.7293(5)	0.5
Nd(3)	2n	0.2732(6)	0.1459(6)	0.5
Cu(1)	1a	0.0	0.0	0.0
Cu(2)	2m	0.166(1)	0.420(1)	0.0
Cu(3)	2m	0.429(1)	0.830(1)	0.0
O(1)	2m	0.075(7)	0.159(5)	0.0
O(2)	2m	0.366(4)	0.281(4)	0.0
O(3)	2m	0.281(6)	0.611(5)	0.0
O(4)	2m	0.239(6)	0.943(4)	0.0
O(5)	2n	0.154(5)	0.424(5)	0.5
O(6)	2n	0.396(5)	0.824(5)	0.5
O(7)	1b	0.0	0.0	0.5

(b) Selected Bond Distances (Å)

Nd(1)−O(2)	2.821(5) [4×]	Cu(1)−O(1)	1.717(9) [2×]
Nd(1)−O(3)	2.838(7) [4×]	Cu(1)−O(4)	1.88(1) [2×]
Nd(1)−O(5)	2.992(8) [2×]	Cu(1)−O(7)	1.889(1) [2×]
Nd(1)−O(6)	2.950(9) [2×]	Cu(2)−O(1)	2.142(8) [1×]
Nd(2)−O(1)	2.766(8) [2×]	Cu(2)−O(2)	2.065(7) [1×]
Nd(2)−O(3)	2.462(6) [2×]	Cu(2)−O(3)	1.901(9) [1×]
Nd(2)−O(4)	2.741(6) [2×]	Cu(2)−O(5)	1.890(1) [1×]
Nd(2)−O(5)	2.697(9) [1×]	Cu(3)−O(2)	2.057(7) [1×]
Nd(2)−O(5)	2.828(8) [1×]	Cu(3)−O(3)	2.218(9) [1×]
Nd(2)−O(6)	2.480(9) [1×]	Cu(3)−O(4)	2.10(1) [1×]
Nd(2)−O(7)	2.601(1) [1×]	Cu(3)−O(6)	1.894(1) [2×]
Nd(3)−O(1)	2.532(8) [2×]		
Nd(3)−O(2)	2.402(4) [2×]		
Nd(3)−O(4)	2.567(5) [2×]		
Nd(3)−O(5)	2.501(9) [1×]		
Nd(3)−O(6)	2.917(9) [1×]		
Nd(3)−O(6)	2.712(9) [1×]		
Nd(3)−O(7)	2.644(1) [1×]		

given in Table 4. Every $Cu^{III}O_6$ octahedron corner-shares with four $Cu^{II}O_5$ square pyramids in the (001) plane and two $Cu^{III}O_6$ octahedra along the c-axis. In each unit cell, one 12-coordinated Nd atom occupies the A-site of the ideal perovskite cell and four 10-coordinated Nd occupy the pseudohexagonal tunnels. The average Nd−O distance of 2.616 Å for 10-coordinated Nd is slightly shorter than the average La−O distance of 2.679 Å in $LaCuO_{2.6}$. Surprisingly, the average Nd−O distance of 2.877 Å for 12-coordinated Nd is longer than the average La−O distance of 2.808 Å for $LaCuO_{2.6}$. With the exception of Cu(1)−O(1) (1.72 Å), the Cu−O distances range from 1.88 to 2.22 Å and are very similar to those observed in $La_4BaCu_5O_{13}$.[7] A

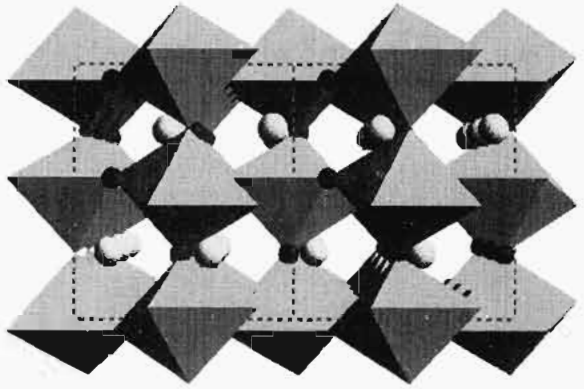

Figure 7. Structure of $NdCuO_{2.93}$ projected on [100]. Large and small balls represent Nd and O atoms, respectively.

Table 5. Positional Parameters and Selected Bond Distances (Å) and Angles (deg) for $NdCuO_{2.93}$

atom	site	x	y	z
Nd	4c	0.0250(8)	0.0961(4)	0.25
Cu	4b	0.5	0.0	0.0
O(1)	4c	0.620(5)	0.975(3)	0.25
O(2)	8d	0.276(4)	0.342(3)	0.054(3)
Nd−O(1)	2.289(5) [1×]	O(1)−Cu−O(1)	180.0(1)	
Nd−O(1)	2.513(4) [1×]	O(1)−Cu−O(2)	94.9(2)	
Nd−O(2)	2.489(4) [2×]	O(1)−Cu−O(2)	88.5(2)	
Nd−O(2)	2.587(4) [2×]	O(1)−Cu−O(2)	91.5(2)	
Nd−O(2)	2.386(4) [2×]	O(1)−Cu−O(2)	85.1(2)	
Cu−O(1)	1.917(2) [2×]			
Cu−O(2)	2.497(4) [2×]			
Cu−O(2)	1.819(5) [2×]			

short Cu−O distance of 1.65 Å was also found in $La_4BaCu_5O_{13}$. The short bond distance could be a result of a distortion of the (001) CuO_2 layer, forcing O(1) and copper to occupy different planes. The symmetry-breaking distortion requires either a doubled c-parameter, consistent with $c \approx 2a_p$ observed by electron diffraction or $P2$ space group. Another possibility is that the coexistence of three perovskite phases in the sample decreases the accuracy of the bond distance determination. The O−Cu−O angles are very variable, spanning the range 76.8−94.0° in $NdCuO_{2.6}$.

Structure of $NdCuO_{2.93}$. Unlike $LaCuO_{3-\delta}$, which exists in both tetragonal[2] and rhombohedral[12] modifications for small δ, $NdCuO_{2.93}$ adopts the perovskite $GdFeO_3$-structure type,[29] with a $\sqrt{2}a_p \times \sqrt{2}a_p \times 2a_p$ supercell. Many $GdFeO_3$-type rare earth oxides have been reported,[28-34] but $NdCuO_{2.93}$ is the first example of a rare earth cation forming the $GdFeO_3$-type perovskite with copper. The structure of $NdCuO_{2.93}$ is shown in Figure 7. The refined positional parameters and selected bond distances and angles for $NdCuO_{2.5}$ are given in Table 5.

Unlike $NdCuO_{2.5}$ and $NdCuO_{2.6}$, the oxygen vacancies are disordered in $NdCuO_{2.93}$. The Nd atom resides in an eight-coordinated bicapped trigonal site with two additional oxygens lying in the Nd plane perpendicular to the c-axis. Eight-coordination of the A-cation is the most common in the $GdFeO_3$-type structure, although the coordination number can vary from 6 to 12.[6,24,28-35] The Nd−O distances range from 2.289 to 2.587 Å, with an average of 2.466 Å. Eight-coordinated Nd also occurs in the T′-type Nd_2CuO_4.[25] The average Nd−O distance of 2.50 Å in T′ is close to that in $NdCuO_{2.93}$. In contrast, the La atom in tetragonal $LaCuO_{2.95}$ is 12-coordinated with an average La−O distance of 2.74 Å. The two *trans* Cu−O bonds of 2.497 Å in $NdCuO_{2.93}$ are much longer than the other four, which range from 1.819 to 1.917 Å. The O−Cu−O angles vary from 87.0 to 94.5°. Such highly distorted octahedra have not been reported in $GdFeO_3$-type compounds. For comparison, there are two *trans* Cu−O bonds at 1.909 Å and four in-plane Cu−O bonds at 1.986 Å in tetragonal $LaCuO_{2.95}$ and six equal bonds at 1.951 Å in rhombohedral $LaCuO_3$.

Conclusions

While five new oxygen-vacancy perovskites have been observed at high pressures in the $NdCuO_{3-\delta}$ system for $0 \leq \delta \leq 0.5$, the attempted synthesis of $LnCuO_{3-\delta}$ failed for Ln = Y, Sm, and Gd, most likely because the A-site atoms are too small to be stabilized in an eight- or higher-coordinated site of cuprate perovskite. The oxygen vacancy ordering found in $NdCuO_{3-\delta}$ depends on δ and the synthetic conditions. As found in the $LaCuO_{3-\delta}$ series, the Cu(II) and Cu(III) cations in the $NdCuO_{3-\delta}$ order in distorted corner-sharing square pyramidal and octahedral sites, respectively. The coordination number of the Nd atom lies between 8 and 12. The $GdFeO_3$-type structure was observed for the first time in the Nd cuprates for $0 \leq \delta \leq 0.07$. While the phases are metallic for $\delta < 0.5$, superconductivity was not observed in $NdCuO_{3-\delta}$ down to 4.2 K. A future study of electric and magnetic properties in the $NdCuO_{3-\delta}$ series could be of interest for comparison with its La homologues.

Although the crystal structures for ordered oxygen-vacancy $NdCuO_{2.5}$ and $NdCuO_{2.6}$ have been determined by X-ray and electron diffraction studies in this work, the structural relationships between $NdCuO_{3-\delta}$ and different $LaCuO_{3-\delta}$ phases, including the unusually short Cu−O distance in $NdCuO_{2.6}$ obtained from the Rietveld refinement are still not quite understood. In order to address these problems, neutron diffraction measurements must be employed. However, it is not yet possible to synthesize enough material for a diffraction experiment in a single high pressure run, and this would be required to ensure the degree of sample homogeneity necessary to obtain accurate neutron data.

Acknowledgment. Work at the LDEO was supported by the National Science Foundation and DOE. Contribution No. 5338 from LDEO.

IC941089A

(28) Maclean, D. A.; Hg, H.-N.; Greendan, J. E. *J. Solid State Chem.* **1979**, *30*, 35.
(29) Geller, S. *J. Chem. Phys.* **1956**, *24*, 1236.
(30) Geller, S. *Acta Crystallogr.* **1957**, *10*, 243.
(31) Geller, S. *Acta Crystallogr.* **1957**, *10*, 248.
(32) Marezio, M.; Remeika, J. P.; Dernier, P. D. *Acta Crystallogr., Sect. B* **1970**, *26*, 2008.
(33) Koopmans, H. J. A.; van De Velde, G. M. H.; Gellings, P. J. *Acta Crystallogr., Sect. C* **1983**, *39*, 1323.
(34) Galasso, F. S. *Structure and Properties of Inorganic Solids*; Pergamon Press: Oxford, England, New York, Toronto, Canada, Sydney, Australia, Braunschweig, Germany, **1970**.
(35) Lelieveld, R.; Ijdo, D. J. W. *Acta Crystallogr., Sect. B* **1980**, *36*, 2223.